Tcf21 as a Founder Transcription Factor in Specifying Foxd1 Cells to the Juxtaglomerular Cell Lineage

Hina Anjum[1], Jason P. Smith[2], Alexandre G Martini[2], George S. Yacu[1], Silvia Medrano[2], R. Ariel Gomez[2], Maria Luisa S. Sequeira-Lopez[2], Susan E. Quaggin[3,4], Gal Finer[1,3*]

[1] Division of Pediatric Nephrology, Ann and Robert H. Lurie Children's Hospital of Chicago, Chicago, IL, USA
[2] Department of Pediatrics, Child Health Research Center, University of Virginia, Charlottesville, VA, USA
[3] Feinberg Cardiovascular and Renal Research Institute, Northwestern University Feinberg School of Medicine, Chicago, IL, USA
[4] Division of Nephrology and Hypertension, Northwestern Memorial Hospital, Chicago IL, USA

*Correspondence: *Gal Finer (gfiner@luriechildrens.org)*

ABSTRACT

Renin is crucial for blood pressure regulation and electrolyte balance, and its expressing cells arise from Foxd1+ stromal progenitors. However, the factors guiding these progenitors toward the renin-secreting cell fate are not fully understood. Tcf21, a basic helix-loop-helix (bHLH) transcription factor, is essential in kidney development. Utilizing *Foxd1*$^{Cre/+}$*;Tcf21*$^{f/f}$ and *Ren1*$^{dCre/+}$*;Tcf21*$^{f/f}$ mouse models, we investigated the role of Tcf21 in the differentiation of Foxd1+ progenitor cells into juxtaglomerular (JG) cells. Immunostaining and in-situ hybridization demonstrated significantly fewer renin-positive areas and altered renal arterial morphology in *Foxd1*$^{Cre/+}$*;Tcf21*$^{f/f}$ kidneys compared with controls, indicating Tcf21's necessity for renin cell emergence. However, Tcf21 inactivation in renin-expressing cells (*Ren1*$^{dCre/+}$*;Tcf21*$^{f/f}$) did not recapitulate this phenotype, suggesting Tcf21 is dispensable once renin cell identity is established.

Integrated analysis of single-cell RNA sequencing (scRNA-seq) and single-cell assay for transposase-accessible chromatin sequencing (scATAC-seq) on GFP+ cells (stromal lineage) from E12, E18, P5, and P30 *Foxd1*$^{Cre/+}$*;Rosa26*^{mTmG} control kidneys revealed that Tcf21 expression peaks at embryonic day 12, crucial for early JG cell specification. Subsequent analyses confirmed Tcf21's critical role in early kidney development, with expression declining as development progresses. Our results highlight the temporal and spatial dynamics of Tcf21, showing its importance in the early specification of Foxd1+ cells into JG cells.

These findings provide new insights into the molecular mechanisms governing JG cell differentiation and underscore Tcf21's pivotal role in kidney development. The data suggest that Tcf21 expression in Foxd1+ progenitors is essential for the specification of renin-expressing JG cells, but once renin cell identity is assumed, Tcf21 becomes redundant.

NEW & NOTEWORTHY

This manuscript provides novel insights into the role of Tcf21 in the differentiation of Foxd1+ cells into JG cells. Utilizing integrated scRNA-seq and scATAC-seq, the study reveals that Tcf21 expression is crucial during early embryonic stages, with its peak at embryonic day 12. The findings demonstrate that inactivation of Tcf21 leads to fewer renin-positive areas and altered renal arterial morphology, underscoring the importance of Tcf21 in the specification of renin-expressing JG cells and kidney development.

Keywords: Foxd1+ stromal progenitors, Tcf21, renin, kidney development

INTRODUCTION

Juxtaglomerular (JG) cells are specialized smooth muscle cells located in the walls of the kidney's afferent arterioles, playing a crucial role in regulating blood pressure and fluid balance through the secretion of renin (1-3). The differentiation of these cells from their progenitors is a tightly regulated process, involving various

transcription factors (4-6). Renin cells originate during kidney development from the stromal progenitors, the Forkhead box D1 positive (Foxd1+) cells, within the metanephric mesenchyme, around embryonic day 13.5 (E13.5) of the mouse. Tcf21, a member of the basic helix-loop-helix (bHLH) transcription factor family, has been implicated in the development of several mesenchymal cell lineages, including those in the kidney (7, 8). However, its specific role in the differentiation of Foxd1+ progenitor cells into JG cells remains unclear. Foxd1 is a transcription factor critical for the formation and differentiation of renal stromal cells, which give rise to several cell types, including JG cells (9-11). Previous studies have demonstrated that Foxd1+ progenitors are essential for kidney morphogenesis and vascular development (9). Given the known roles of Tcf21 and Foxd1 in kidney development, it is hypothesized that Tcf21 may play a pivotal role in the differentiation of Foxd1+ cells into JG cells. This study aims to elucidate the role of Tcf21 in the specification and differentiation of Foxd1+ progenitor cells into renin-expressing JG cells. Utilizing *Foxd1*$^{Cre/+}$*;Tcf21*$^{f/f}$ and *Ren1*$^{dCre/+}$*;Tcf21*$^{f/f}$ mouse models, histological analysis and integrated scRNA-seq) and scATAC-seq) analysis, we investigated the temporal and spatial dynamics of Tcf21 expression in these cells across various developmental stages. Our results indicate that Tcf21 is crucial for the early specification of Foxd1+ cells into JG cells, with its expression peaking during the early embryonic stage and declining as development progresses. This study provides new insights into the molecular mechanisms governing JG cell differentiation and highlights the importance of Tcf21 in kidney development.

MATERIALS AND METHODS

Mice and genotyping

All mouse experiments were approved by the Animal Care Committee at the Center for Comparative Medicine of Northwestern University (Evanston, IL) and were performed in accordance with institutional guidelines and the NIH Guide for the Care and Use of Laboratory Animals. The *Tcf21*$^{floxf/lox}$ and *Ren1*$^{dCre/+}$mice were created as previously described (12, 13). The *Foxd1-eGFPCre* mice were kind gifts from Dr. Andrew McMahon (University of Southern California) and are described elsewhere (14). Genotyping was performed with Quick-Load Taq 2X Master Mix (M0271L, BioLabs), on 2% agarose gel for the PCR bands. Primer information is in **Suppl. Table 1**.

Histology, immunohistochemistry and immunofluorescence

Mouse embryo dissections were performed at the indicated time-points. Samples were fixed with 10% Neutral buffered formalin or 4% paraformaldehyde overnight, embedded in paraffin, and sectioned into 5µm by the Mouse Histology and Phenotyping Laboratory (MHPL) of Northwestern University. Sections were deparaffinized in xylene and ethanol and boiled in citrate buffer for antigen retrieval. Sections were then treated with 1% donkey serum with 0.3% TritonX100 in PBS for 30 minutes at room temperature before incubating with primary antibodies at 4°C overnight. Sections were washed in PBS and incubated with Alexa Fluor fluorescence-conjugated secondary antibodies for 45 minutes at room temperature. Antibody information: CD31 (R&D, AF3628, 1:200) and CD146 (abcam, ab75769, 1:200), Krt8 (TROMA-I-s, DSHB. 1:20), Renin (Alpha Diagnostic, Gomez project 1:500). All secondary antibodies were purchased from Molecular Probes ThermoFisher Scientific and used at a 1:500 dilution. For 5 channel imaging, secondary antibodies were employed as follows: AlexaFluor 488, 555, 594, 647 and DAPI.

In-situ hybridization (RNAScope)

In-situ hybridization was performed on paraffin section using RNAscope (15) and following ACD® protocol https://acdbio.com/rnascope-25-hd-duplex-assay. Probes: Tcf21 (ACD #508661), Ren1 (ACD #433461).

Isolation of kidney single cells: E12

Pregnant mice were anesthetized with tribromoethanol. Small fetuses were removed, and GFP pups were identified using the EvosFLC cell imaging system (LifeTechnologies, California, USA). The metanephros area was dissected, minced, and incubated in TryPLE Express (Gibco, New York, USA) at 37°C for 5 minutes. After adding DMEM + 5% FBS, the mixture was homogenized and filtered through a 40 µm nylon cell strainer. The filtrate was centrifuged, and the pellet resuspended in resuspension buffer, preparing cells for single-cell capture. n=15 (E12, both sexes represented based on Mendelian ratios).

Isolation of Kidney Single Cells: E18, P5, and P30

Animals were anesthetized with tribromoethanol (300 mg/kg). Kidneys from P5 and P30 mice were excised, decapsulated, and dissected. The kidney cortices were minced and digested in an enzymatic solution (0.3% collagenase A, 0.25% trypsin, 0.0021% DNase I) in a shaking incubator (80 RPM) at 37°C for 15 minutes. The supernatant was collected, and the digestion was repeated three times. The pooled supernatants were centrifuged, and the pellet resuspended in buffer 1 (130 mM NaCl, 5 mM KCl, 2 mM CaCl2, 10 mM glucose, 20 mM sucrose, 10 mM HEPES, pH 7.4), filtered through 100 µm and 40 µm nylon cell strainers, and centrifuged again. The final pellet was resuspended in resuspension buffer, DAPI added, and GFP positive cells were sorted by FACS (Influx Cell Sorter or FACS Aria Fusion Cell Sorter, Becton Dickinson) and resuspended in DMEM with 10% FBS for immediate use. n=18 (E18, both sexes represented based on Mendelian ratios), n=12 (P5, 6 females and 6 males), and n=10 (P30, 4 females and 6 males).

scATAC-seq Library Preparation

GFP-positive cells were washed in dPBS with 0.04% BSA and counted with a CellometerMini (Nexcelom Bioscience, Massachusetts, USA). Cells with over 80% viability were processed for nuclei isolation using Low Cell Input Nuclei Isolation protocol. Cells were lysed, washed, and nuclei counted with a Neubauer Chamber (Spencer, Buffalo, USA). Nuclei were captured using the Chromium System (10X Genomics) and processed for sequencing on an Illumina HiSeq platform.

scRNA-seq Library Preparation

GFP-positive cells were spun down and resuspended in dPBS with 0.04% BSA, counted, and processed with the Chromium System (10X Genomics) following the manufacturer's recommendations. Barcoded cDNA was amplified and sequenced on an Illumina HiSeq platform.

Read Preprocessing

Genome and transcriptome annotations were performed using the mm10 genome. Cell Ranger pipeline (refdata-cellranger-arc-mm10-2020-A-2.0.0) and BSgenome package (BSgenome.Mmusculus.UCSC.mm10) were used.

scATAC-seq Analysis

FASTQ files were processed with Cell Ranger ATAC (cellranger-atac-2.0.0), and duplicate reads were removed. ArchR v1.0.1 was used for quality control, dimensionality reduction, batch correction (Harmony algorithm), and cell clustering. Pseudo-bulk replicates were generated for peak calling using MACS2.

scRNA-seq Analysis

FASTQ files were processed with Cell Ranger (cellranger-6.0.1). Feature-barcode matrices were analyzed with Seurat for normalization, PCA, clustering, and cell identification using marker genes. Integration of scRNA-seq and scATAC-seq data was performed using ArchR's addGeneIntegrationMatrix function.

Renin Cell Differentiation Trajectory

Trajectory inference identified dynamic chromatin and expression changes from FoxD1+ progenitor cells to renin cells using ArchR's addTrajectory function. Mature renin cells were identified by filtering for specific markers, and subpopulations were analyzed for chromatin accessibility and motif enrichment. Gene scores, which estimate gene activity by proxy of chromatin accessibility, were calculated by summing reads in peaks with the nearest annotated gene.

RESULTS

Inactivation of *Tcf21* in Foxd1+ cells leads to fewer renin-positive areas in the developing kidney.

Utilizing the *Foxd1*$^{Cre/+}$;*Tcf21*$^{f/f}$ mouse in which *Tcf21* is excised in Foxd1+ cells (16), we initially examined renin protein expression by immunostaining. At mid- and late-stages of kidney development (i.e., E16.5 and E18.5), *Tcf21* stromal conditional knockout (*Tcf21* stromal cKO) demonstrated globally fewer renin-positive areas, representing lower renin expression in juxtaglomerular apparatus and arteriolar walls, compared with controls (**Fig.1 IA-C**). Morphologic examination of the developing afferent arterioles, where renin cells normally reside, revealed thinner and shorter walls in the E16.5 *Tcf21* stromal cKO compared with controls (**Fig.1 IIA-C**). To further corroborate this finding, we performed immunostaining for renin and the melanoma cell adhesion molecule (MCAM, CD146), a marker of perivascular cells (e.g. pericytes, VSMC) (17-19). This staining revealed reduced renin and MCAM expression in the walls of the afferent arterioles in *Tcf21* stromal cKO compared with

control (**Fig.1 IIIA-C**). This renin+MCAM+ cell population has been previously characterized as renin-positive pericytes that are believed to represent a specialized subpopulation known for their pericyte role in supporting vessel formation and for their distinct ability to synthesize renin (2, 20). Next, we examined the medullary peritubular capillaries, where we observed again a marked reduction in renin and MCAM signals in *Tcf21 stromal* cKO compared with control (**Fig.1 IIID-F**).

Complementarily, we evaluated renin mRNA expression at early-, mid-, and late-stages of nephrogenesis (i.e., E14.5, E16.5, and E18.5) in control and *Tcf21* stromal cKO. Using in-situ hybridization (RNAscope), we detected a strong *Renin* signal in the arterioles leading into the developing glomeruli of control kidneys at E16.5 and E18.5 (**Fig.2 IA-B, IIA-C**). *Renin* expressing cells were primarily distributed in aggregates along the corticomedullary junction where newly formed glomeruli are known to mature (**Fig.2 IA**). In-line with the previously reported normal emergence of renin-expressing cells around E13.5 of the developing mouse kidney, we detected a scattered patten of *Renin* expression at E14.5 of control kidneys which was less robust compared with *renin* expression at E16.5 and E18.5 (**Fig.2 IIE,F**). In contrast to controls, *Renin* mRNA expression in *Tcf21* stromal cKO kidneys was reduced, showing fewer *Renin*-positive areas, although cells expressing renin mRNA were still present in some pre-glomerular arterioles (**Fig.2 IA',B', IIA'-F'**).

As to *Tcf21* expression in controls, as previously described (16), we detected robust *Tcf21* signal throughout stromal regions surrounding the cortex, sub-cortex, medulla, papilla, and ureter (**Fig.2 IIA,C,E**). In addition to the stroma, a strong Tcf21 signal was detected in podocytes at E16.5 and E18.5, and in segments of developing nephron structures at E14.5 (**Fig.2 IIB,D,F**). On the other hand, $Foxd1^{Cre/+};Tcf21^{f/f}$ kidneys showed marked reduction in *Tcf21* expression in the stroma, but its expression was still detected in some regions of the medullary stroma (**Fig.2 IIC'**), which could be explained by incomplete Cre-mediated excision of *Tcf21* in a population of stromal cells. As expected, we detected *Tcf21* signal in podocytes, developing nephrons, and in the ureteric stromal of the mutants, as these cells are not progeny of the Foxd1+ lineage but originate from the Six2 and Tbx18 lineages (21, 22). Taken together, these results suggest that expression of *Tcf21* in Foxd1+ cells is required for normal expression of renin mRNA and protein with ramifications to the development of the afferent arterioles.

Inactivation of *Tcf21* under the *Renin* promotor does not recapitulate the vascular phenotype of $Foxd1^{Cre/+};Tcf21^{f/f}$

The vascular defect seen in *Tcf21* stromal cKO kidneys brought up the possibility that continuous *Tcf21* expression in JG cells might be necessary for normal arterial development. To test this, we inactivated *Tcf21* in renin-expressing cells by breeding $Tcf21^{f/f}$ mice with $Ren1^{dCre/+}$ mice (13, 23, 24), creating the $Ren1^{dCre/+};Tcf21^{f/f}$ (*Tcf21* renin cKO) mouse. Using immunostaining with the pan-endothelial marker PECAM (CD31) and 3D image analysis of cleared E16.5 kidneys, we observed no difference in vascular morphology between the *Tcf21* renin cKO and controls (**Fig.3 I, Suppl. Fig.1**). In contrast, *Tcf21* stromal cKO kidneys displayed fewer, shorter, and thinner branches (**Fig.3 I** and (16)). This suggests that once Foxd1+ cells become renin cells, *Tcf21* expression is no longer needed for kidney vasculature formation. Evaluating the morphology of the $Ren1^{dCre/+};Tcf21^{f/f}$ kidneys in two- and four-month-old mice showed normal renal architecture and vessel morphology compared with controls (**Fig.3 IIA-**, **Suppl. Fig.2**), indicating Tcf21 is dispensable once renin cell identity is established.

To test if Tcf21 regulates renin expression, we compared renin positive spots in $Ren1^{dCre/+};Tcf21^{f/f}$ and control kidneys using in-situ hybridization. In two-month-old mice, *Tcf21* renin cKO kidneys showed similar renin mRNA expression pattern as controls (**Suppl. Fig.3**). Similarly, at E14.5, Tcf21 and renin mRNA signals did not co-localize (**Suppl. Fig.4**), suggesting *Tcf21*'s regulatory action is completed before renin promoter activation.

Temporal and spatial dynamics of Tcf21 expression in the differentiation of Foxd1+ cells into juxtaglomerular cells

To investigate the role of Tcf21 in the differentiation of Foxd1+ cells into JG cells, we analyzed integrated scRNA-seq and scATAC-seq data from 6,191 GFP+ cells (stromal lineage) purified via flow cytometry from $Foxd1^{Cre/+};Rosa26^{mTmG}$ control kidneys across various developmental stages. Our aim was to elucidate the temporal and spatial expression patterns of *Tcf21* and its impact on the specification of renin-expressing cells.

We bioinformatically identified the JG lineage by selecting Foxd1-expressing cells with high *Ren1* and *Akr1b7* expression and chromatin accessibility scores from P5 to P30 (N=2,054). Using trajectory inference with ArchR, we calculated pseudotime trajectories to map the dynamic chromatin and expression changes from Foxd1+

progenitor cells to renin-expressing cells. These trajectories were visualized on UMAP embeddings for further analysis. *Tcf21* expression was examined in JG cells at E12, E18, postnatal day 5 (P5), and P30.

A violin plot of *Tcf21* expression levels in [log2 (normcounts + 1)] across these four key developmental timepoints indicated a clear trend of decreasing *Tcf21* expression from E12 to P30 (**Fig. 4A**). At E12, *Tcf21* shows relatively high expression with moderate variability. By E18, *Tcf21* expression dropped notably. The data for E18 also showed a wide spread of *Tcf21* expression values, suggesting diverse regulatory processes during this stage. P5 showed a further decrease in *Tcf21* expression, reflecting continued downregulation of *Tcf21* after birth. By P30, reflecting mature kidneys, *Tcf21* expression level remained low. The histogram of *Tcf21* expression levels in JG cells split by developmental stages showed that E12 cells predominated at intermediate expression levels and were scarce at lower levels (**Fig. 4B**). This implies that *Tcf21* expression is more prevalent during E12, supporting its critical role in early development and initial differentiation. Quartile analysis confirmed this trend, showing that E12 cells exclusively expressed Tcf21 above the second quartile. Furthermore, the majority of these cells expressed Tcf21 at or above the third quartile, which contrasts sharply with later developmental stages where most cells exhibited Tcf21 expression at minimum levels, up to the second quartile (**Fig. 4C**). Uniform Manifold Approximation and Projection (UMAP) visualization highlights annotated cell populations that define the trajectory leading to mature JG cells across developmental stages (**Fig. 4D, E**). Temporal (pseudotime trajectory) and cell-type changes in Tcf21 expression revealed higher expression in clusters 1, 2, and 3 corresponding to metanephric mesenchyme, stromal progenitors, and renin precursors (**Fig. 4F-G**). Motif enrichment and pseudotime trajectory analyses further underscored Tcf21's role in early kidney development (**Fig. 4H**), emphasizing its crucial role in the early specification of Foxd1+ cells into JG cells. These findings align with previous results showing reduced renin-positive areas and altered renal arterial tree morphology in *Tcf21* stromal cKO mice, underscoring the importance of Tcf21 in kidney development and JG cell lineage specification.

Overall, these data suggest that Tcf21 is highly active during early stages of kidney development in metanephric mesenchyme, stromal progenitors, and renin precursors, gradually decreasing as development progresses and the organ matures. This pattern supports the hypothesis that Tcf21 is crucial for early specification and differentiation processes within the kidney, diminishing in importance as these processes near completion.

DISCUSSION

The developmental pathways that guide the differentiation of Foxd1+ stromal progenitors into various cell types, such as JG cells, are crucial for proper kidney morphogenesis and function. Our study elucidates the role of Tcf21 in the differentiation of Foxd1+ progenitor cells into JG cells during kidney development. The results demonstrate that Tcf21 expression is essential for the early specification of these progenitors into renin-expressing JG cells, with its expression peaking during early embryogenesis and diminishing as development progresses. The inactivation of Tcf21 in Foxd1+ cells led to a significant reduction in renin-positive areas within the developing kidney. This was evident through the decreased renin protein and mRNA expression, as well as the morphological alterations in the afferent arterioles. The reduced renin and MCAM expression in the *Tcf21* stromal cKO suggests that Tcf21 is necessary for the proper differentiation and function of renin-expressing pericytes, which play a critical role in vessel formation and renin synthesis. Our findings align with previous research indicating the importance of Foxd1+ progenitors in kidney morphogenesis and vascular development. The temporal and spatial dynamics of Tcf21 expression revealed through integrated scRNA-seq and scATAC-seq analyses further underscore its role in the early stages of kidney development. The gradual decrease in Tcf21 expression from E12 to P30 supports the hypothesis that Tcf21 is vital during the initial stages of JG cell specification and differentiation. Interestingly, the inactivation of Tcf21 under the renin promoter did not replicate the vascular phenotype observed in the $Foxd1^{Cre/+};Tcf21^{f/f}$ model. This indicates that once Foxd1+ cells commit to the renin-expressing lineage, Tcf21 is no longer required for vascular development. The normal renal architecture and vessel morphology in mature *Tcf21* renin cKO kidneys further support this notion, suggesting that Tcf21's role is primarily confined to the early stages of cell fate determination. Our motif enrichment and pseudotime trajectory analyses highlight Tcf21's influence in early kidney development, particularly in the metanephric mesenchyme, stromal progenitors, and renin precursors. These findings provide new insights into the molecular mechanisms governing JG cell differentiation and emphasize the role of Tcf21 in the early specification of Foxd1+ cells into JG cells.

It is important to mention that the variability in Tcf21 deletion among cells, which may have resulted from non-absolute Cre-mediated recombination, possibly affected the uniformity of our findings. Additionally, this study did not address the complexity of the transcriptional networks governing Foxd1+ cell differentiation in terms of identifying Tcf21 binding partners, coregulators, and direct targets. These aspects should be explored in future research and could have functional implications. Finally, we did not explore potential compensatory mechanisms that might mitigate the effects of Tcf21 deficiency on JG cell differentiation. Although we did not consistently determine the sex of the mice in every experiment, and there was variability in the representation of each sex across different experiments, both preliminary and subsequent analyses consistently demonstrated a vascular phenotype in both male and female *Foxd1*$^{Cre/+}$*;Tcf21*$^{f/f}$ and the absence of one in *Ren1*$^{dCre/+}$*;Tcf21*$^{f/f}$ mice. To account for potential sex-related effects, we utilized age-matched male and female cohorts, selecting them based on availability at the time of each experiment. Furthermore, our preliminary data and additional experiments, not included in this manuscript, did not reveal any significant gross morphological differences between the sexes.
In summary, our study highlights the complexity of transcriptional regulation in the specification and maintenance of the JG cell lineage. Tcf21 may prime cis-regulatory elements in a cell- and developmental stage-specific manner to control the specification of various stromal sub-populations. Further work is required to construct a comprehensive spatial and temporal developmental atlas of stromal cells during kidney development. By uncovering Tcf21's role in early specification and its dispensability in later stages, we lay a foundation for further research into key signaling pathways and mechanisms in renal vascular development.

DATA AVAILABILITY

Data is publicly available at Gene Expression Omnibus (GSE218570).

SUPPLEMENTAL MATERIAL

Supplemental Figures 1-4:

Suppl Fig. 1: Tissue clearing and immunostaining of *Ren1*$^{dCre/+}$*;Tcf21*$^{f/f}$. n=4, females.

Suppl Fig. 2: Histology of two-month old mice of control and *Ren1*$^{dCre/+}$*;Tcf21*$^{f/f}$ kidneys. n=16, females.

Suppl Fig. 3: Normal *renin* mRNA expression in *Ren1*$^{dCre/+}$*;Tcf21*$^{f/f}$ mouse kidney at 2 months.

Suppl Fig. 4: RNAScope of *Tcf21* and *renin* at E14.5 control kidneys. n=2, unknown sex.

Supplemental Table 1:

Suppl Table 1: Primer information (genotyping)

ACKNOWLEDGMENTS

Confocal microscopy was provided by the Center for Advanced Microscopy of Northwestern University and by the Microscopy and Histology Group at Stanley Manne Children's Research Institute affiliated with Ann and Robert H. Lurie Children's Hospital of Chicago. With gratitude to the Zell Family Foundation.

Author contributions: G.F., M.L.S.S.L., R.A.G., A.G.M., and S.E.Q. designed the study; G.F., H.A., and A.G.M., carried out experiments; G.F., M.L.S.S.L., R.A.G., J.P.S., and H.A., analyzed the data; G.F., and G.Y., made the figures; G.F., M.L.S.S.L.,R.A.G., J.P.S., and S.E.Q. drafted and revised the paper; all authors approved the final version of the manuscript.

GRANTS

National Institutes of Health, National Institutes of Diabetes and Digestive and Kidney Diseases, K08 DK-118180 (to Gal Finer). National Institutes of Health, UVA Pediatric Center of Excellence in Nephrology, P50 DK-096373 (to Gal Finer).

DISCLOSURES

Susan E. Quaggin holds patents related to therapeutic targeting of the ANGPT-TEK pathway in ocular hypertension and glaucoma and owns stock in and is a director of Mannin Research. S. Quaggin also receives consulting fees from AstraZeneca, Janssen, the Lowy Medical Research Foundation, Roche/Genentech, Novartis,

and Pfizer and is a scientific advisor or member of AstraZeneca, Genentech/Roche, JCI, the Karolinska CVRM Institute, the Lowy Medical Research Institute, Mannin, Novartis and Goldilocks. All other authors have nothing to disclose.

REFERENCES

1. **Sequeira-Lopez MLS, and Gomez RA**. Renin Cells, the Kidney, and Hypertension. *Circ Res* 128: 887-907, 2021.
2. **Sequeira Lopez ML, and Gomez RA**. Development of the renal arterioles. *J Am Soc Nephrol* 22: 2156-2165, 2011.
3. **Reddi V, Zaglul A, Pentz ES, and Gomez RA**. Renin-expressing cells are associated with branching of the developing kidney vasculature. *J Am Soc Nephrol* 9: 63-71, 1998.
4. **Gomez RA, Pentz ES, Jin X, Cordaillat M, and Sequeira Lopez ML**. CBP and p300 are essential for renin cell identity and morphological integrity of the kidney. *Am J Physiol Heart Circ Physiol* 296: H1255-1262, 2009.
5. **Smith DL, Morris BJ, Do YS, Law RE, Shaw KJ, and Hseuh WA**. Identification of cyclic AMP response element in the human renin gene. *Biochem Biophys Res Commun* 200: 320-329, 1994.
6. **Pan L, Black TA, Shi Q, Jones CA, Petrovic N, Loudon J, Kane C, Sigmund CD, and Gross KW**. Critical roles of a cyclic AMP responsive element and an E-box in regulation of mouse renin gene expression. *J Biol Chem* 276: 45530-45538, 2001.
7. **Tandon P, Miteva YV, Kuchenbrod LM, Cristea IM, and Conlon FL**. Tcf21 regulates the specification and maturation of proepicardial cells. *Development* 140: 2409-2421, 2013.
8. **Acharya A, Baek ST, Huang G, Eskiocak B, Goetsch S, Sung CY, Banfi S, Sauer MF, Olsen GS, Duffield JS, Olson EN, and Tallquist MD**. The bHLH transcription factor Tcf21 is required for lineage-specific EMT of cardiac fibroblast progenitors. *Development* 139: 2139-2149, 2012.
9. **Sequeira-Lopez ML, Lin EE, Li M, Hu Y, Sigmund CD, and Gomez RA**. The earliest metanephric arteriolar progenitors and their role in kidney vascular development. *Am J Physiol Regul Integr Comp Physiol* 308: R138-149, 2015.
10. **Song R, Lopez M, and Yosypiv IV**. Foxd1 is an upstream regulator of the renin-angiotensin system during metanephric kidney development. *Pediatr Res* 82: 855-862, 2017.
11. **Kragesteen BK, Giladi A, David E, Halevi S, Geirsdottir L, Lempke OM, Li B, Bapst AM, Xie K, Katzenelenbogen Y, Dahl SL, Sheban F, Gurevich-Shapiro A, Zada M, Phan TS, Avellino R, Wang SY, Barboy O, Shlomi-Loubaton S, Winning S, Markwerth PP, Dekalo S, Keren-Shaul H, Kedmi M, Sikora M, Fandrey J, Korneliussen TS, Prchal JT, Rosenzweig B, Yutkin V, Racimo F, Willerslev E, Gur C, Wenger RH, and Amit I**. The transcriptional and regulatory identity of erythropoietin producing cells. *Nat Med* 29: 1191-1200, 2023.
12. **Maezawa Y, Onay T, Scott RP, Keir LS, Dimke H, Li C, Eremina V, Maezawa Y, Jeansson M, Shan J, Binnie M, Lewin M, Ghosh A, Miner JH, Vainio SJ, and Quaggin SE**. Loss of the podocyte-expressed transcription factor Tcf21/Pod1 results in podocyte differentiation defects and FSGS. *J Am Soc Nephrol* 25: 2459-2470, 2014.
13. **Mohamed TH, Watanabe H, Kaur R, Belyea BC, Walker PD, Gomez RA, and Sequeira-Lopez MLS**. Renin-Expressing Cells Require beta1-Integrin for Survival and for Development and Maintenance of the Renal Vasculature. *Hypertension* 76: 458-467, 2020.
14. **Kobayashi A, Mugford JW, Krautzberger AM, Naiman N, Liao J, and McMahon AP**. Identification of a multipotent self-renewing stromal progenitor population during mammalian kidney organogenesis. *Stem Cell Reports* 3: 650-662, 2014.
15. **Wang F, Flanagan J, Su N, Wang LC, Bui S, Nielson A, Wu X, Vo HT, Ma XJ, and Luo Y**. RNAscope: a novel in situ RNA analysis platform for formalin-fixed, paraffin-embedded tissues. *J Mol Diagn* 14: 22-29, 2012.
16. **Finer G, Maezawa Y, Ide S, Onay T, Souma T, Scott R, Liang X, Zhao X, Gadhvi G, Winter DR, Quaggin SE, and Hayashida T**. Stromal Transcription Factor 21 Regulates Development of the Renal Stroma via Interaction with Wnt/beta-Catenin Signaling. *Kidney360* 3: 1228-1241, 2022.

17. **Chen J, Luo Y, Hui H, Cai T, Huang H, Yang F, Feng J, Zhang J, and Yan X**. CD146 coordinates brain endothelial cell-pericyte communication for blood-brain barrier development. *Proc Natl Acad Sci U S A* 114: E7622-E7631, 2017.
18. **Manocha E, Consonni A, Baggi F, Ciusani E, Cocce V, Paino F, Tremolada C, Caruso A, and Alessandri G**. CD146(+) Pericytes Subset Isolated from Human Micro-Fragmented Fat Tissue Display a Strong Interaction with Endothelial Cells: A Potential Cell Target for Therapeutic Angiogenesis. *Int J Mol Sci* 23: 2022.
19. **Espagnolle N, Guilloton F, Deschaseaux F, Gadelorge M, Sensebe L, and Bourin P**. CD146 expression on mesenchymal stem cells is associated with their vascular smooth muscle commitment. *J Cell Mol Med* 18: 104-114, 2014.
20. **Castrop H, Hocherl K, Kurtz A, Schweda F, Todorov V, and Wagner C**. Physiology of kidney renin. *Physiol Rev* 90: 607-673, 2010.
21. **Kobayashi A, Valerius MT, Mugford JW, Carroll TJ, Self M, Oliver G, and McMahon AP**. Six2 defines and regulates a multipotent self-renewing nephron progenitor population throughout mammalian kidney development. *Cell Stem Cell* 3: 169-181, 2008.
22. **Bohnenpoll T, Bettenhausen E, Weiss AC, Foik AB, Trowe MO, Blank P, Airik R, and Kispert A**. Tbx18 expression demarcates multipotent precursor populations in the developing urogenital system but is exclusively required within the ureteric mesenchymal lineage to suppress a renal stromal fate. *Dev Biol* 380: 25-36, 2013.
23. **Belyea BC, Xu F, Pentz ES, Medrano S, Li M, Hu Y, Turner S, Legallo R, Jones CA, Tario JD, Liang P, Gross KW, Sequeira-Lopez ML, and Gomez RA**. Identification of renin progenitors in the mouse bone marrow that give rise to B-cell leukaemia. *Nat Commun* 5: 3273, 2014.
24. **Sequeira Lopez ML, Pentz ES, Nomasa T, Smithies O, and Gomez RA**. Renin cells are precursors for multiple cell types that switch to the renin phenotype when homeostasis is threatened. *Dev Cell* 6: 719-728, 2004.

FIGURE LEGENDS

Figure 1: **Inactivation of Tcf21 in Foxd1+ cells results in lower renin expression at E16.5 and E18.5.** I. A, A', representative E16.5 kidney of *Foxd1*$^{Cre/+}$*;Tcf21*$^{f/f}$ shows lower renin expression level (brown staining) compared to control. Scale bar 200µm. n=4. B, B', JG area of a glomerulus of *Tcf21* stromal cKO demonstrates reduced renin expression compared with control. (IHC on H&E staining). Scale bar 20µm. n=6, sex not determined. C, quantification of the number of renin-expressing cell aggregates (renin positive areas) in controls and *Tcf21* stromal cKO kidneys at E18.5. II. A, A', B, B', and C, C', the afferent arteriole of the glomerulus, stained for CD31+ (PECAM) endothelial cells and CD146+ (MCAM) pericytes, is thinner and shorter in *Tcf21* stromal cKO compared with control. Scale bar 50µm. 3D imaging in (16). n=12, sex not determined. III. A-C, reduced CD146+Renin+ staining along the afferent arteriole of *Tcf21* stromal cKO compared with control. D-F, peritubular capillaries in the medulla show lower renin+ pericytes in *Foxd1*$^{Cre/+}$*;Tcf21*$^{f/f}$ kidneys compared with control. Scale bar 50µm. n=4. Sex not determined.

Figure 2: **Reduced renin mRNA expression in the developing kidney of *Tcf21* stromal cKO.** *In-situ hybridization (RNAscope).* I. A, A', B, B', at E18.5, control kidney express *renin* in cells of the afferent arterioles and in the hilum of the glomerulus along the corticomedullary junction, while *Foxd1*$^{Cre/+}$*;Tcf21*$^{f/f}$ kidneys demonstrate lower renin expression (quantification in II). n=4. II A-F, control kidneys at E14.5 through E18.5 demonstrate robust Tcf21 expression (purple) in the stroma and glomeruli, and *renin* expression (blue) along the afferent arterioles leading to the kidney hilum. A'-F' *Foxd1*$^{Cre/+}$*;Tcf21*$^{f/f}$ kidneys show a marked reduction in *Tcf21* expression in the majority of the stroma. Tcf21 expression is intact in the glomeruli and stroma surrounding the ureter, cells that originate from Six2 and Tbx18 progenitors. Renin expression is diminished in the JG regions of *Tcf21* stromal cKO. Scale bar 100µm. n=4 at each timepoint. Sex not determined.

Figure 3: Inactivation of Tcf21 upon renin promoter expression does not recapitulate the vascular phenotype of *Foxd1*$^{Cre/+}$*;Tcf21*$^{f/f}$ kidneys.

I. Immunostaining for CD31 (PECAM, pan-endothelial) and Keratin8 (ureteric bud) demonstrates the arterial tree of E16.5 *Ren1*$^{dCre/+}$*;Tcf21*$^{f/f}$ (left) and E15.5 *Foxd1*$^{Cre/+}$*;Tcf21*$^{f/f}$ (right) kidneys and controls. A,A', the *Ren1*$^{dCre/+}$*; Tcf21*$^{f/f}$ shows vascular patterning that is unchanged compared with control (3D visualization in **Suppl Fig. 1**). n=8, 6 males, 2 females. B, B', in contrast, the arterial tree of *Foxd1*$^{Cre/+}$*;Tcf21*$^{f/f}$ kidneys demonstrates distorted pattern with disorganized, shorter, and thinner arterioles that display abnormal centripetal pattern with abnormal vessel branching of an aberrant ramification leading into the capsule (described in detail in (16)). Scale bar 100 µm. n=6, females. II. Histology of four month old of *Ren1*$^{dCre/+}$*; Tcf21*$^{f/f}$ kidneys does not show phenotypic changes upon H&E (left), and Trichrome (right) staining compared with controls. At 4 months, similar to the findings at E15.5, the morphology of the vascular walls and glomeruli appear intact in *Ren1*$^{dCre/+}$*; Tcf21*$^{f/f}$. Scale bar 1000 µm for A-B, 100 µm for C-H. n=4, males.

Figure 4: Distribution of Tcf21 expression from integrated analysis of scRNA-seq and scATAC-seq data.
A-C: Tcf21 expression in Juxtaglomerular (JG) cells at E12, E18, P5, and P30. A. Violin plot showing Tcf21 expression levels (log2 scale) across developmental time points. B. Histogram presenting the number of JG cells across different Tcf21 expression levels (x-axis) divided by developmental time points. C. Tcf21 expression presented in quartile bins across developmental time points. The color coding is as follows: Navy blue: Cells expressing Tcf21 at minimum values up to and including the first quartile. Purple: Cells expressing Tcf21 above the first quartile up to and including the second quartile (median). Red: Cells expressing Tcf21 above the median and up to and including the third quartile. Orange: Cells expressing Tcf21 above the third quartile.
Note the highest Tcf21 expression at E12, with lower expression levels observed at later stages of kidney development (E18, P5) and in the mature kidney (P30).
D-H: Cell type annotation within the JG lineage and Tcf21 expression across distinct JG cells. D. Uniform Manifold Approximation and Projection (UMAP) plot of GFP+ cells (stromal lineage) combined from samples of mouse embryonic kidneys at E12, E18, P5, and P30, projected in two dimensions. Each dot represents a single cell, and each color denotes a cell type annotation within the JG cell lineage. E. UMAP plot as in D, but here each color represents a distinct developmental timepoint. F-G. (Upper plots) Tcf21 RNA expression levels within the JG cell population presented as signal intensity on a log2 scale in F and inferred gene expression from chromatin accessibility (Gene Score) on a log2 scale in G on the corresponding UMAPs. (Lower plots) Corresponding values plotted along the pseudotime of the JG trajectory. Note the higher Tcf21 expression in cells of clusters 1, 2, and 3 (annotated as stromal progenitors, renin precursors, and metanephric mesenchyme progenitors) compared to other clusters. H. (Upper plot) Tcf21 motif enrichment presented as z-scores of the bias-corrected motif deviation values within the JG cell population projected on the UMAP. (Lower plots) Corresponding values plotted along the pseudotime of the JG trajectory. n=15 (E12), n=18 (E18), n=12 (P5), and n=10 (P30). Both sexes represented based on Mendelian ratios.

LEGENDS FOR SUPPLAMENTRAY FIGURE

Suppl Figure 1: Tissue clearing and immunostaining of kidneys from *Ren1*$^{dCre/+}$*;Tcf21*$^{f/f}$ and controls. Babb clearing, immunostaining with the pan-endothelial marker PECAM (CD31; red), and 3D imaging show no difference in vascular morphology between *Ren1*$^{dCre/+}$*;Tcf21*$^{f/f}$ and control kidneys at E16.5. n=4, females.

Suppl Figure 2: Histology from 2-month-old *Ren1*$^{dCre/+}$*;Tcf21*$^{f/f}$ and control kidneys. H&E (top) and Trichome (bottom) stainings reveal no gross phenotypic changes in *Ren1*$^{dCre/+}$*;Tcf21*$^{f/f}$ kidneys compared with controls. Vascular wall and glomeruli morphology appear intact. Scale bar 100 µm. n=16, females.

Suppl Figure 3: **Normal *renin* mRNA expression *Ren1*$^{dCre/+}$*;Tcf21*$^{f/f}$ kidneys at 2 months.**
In-situ hybridization *(RNAscope).* A,A', B,B' *Renin* expression (blue) is detected in the arteriolar walls (yellow arrows) and in the glomerulus hilum (black arrows) similarly in 2-month-old *Ren1*$^{dCre/+}$*; Tcf21*$^{f/f}$ and control kidneys. C,C', The distribution of renin-expressing cells is similar in *Ren1*$^{dCre/+}$*; Tcf21*$^{f/f}$ and controls. Scale bar 75µm (A), 100µm (B,C). n=4, females.

Suppl Figure 4: In-situ hybridization of Tcf21 and renin in E14.5 *Ren1*$^{d+/+}$*;Tcf21*$^{f/f}$ kidneys. In-situ hybridization (*RNAscope*) shows no co-localization of *Tcf21* (purple) and *renin* (blue) mRNA in E14.5 control kidneys. This time point was chosen because renin-expressing cells emerge around E13.5. n=2, unknown sex.

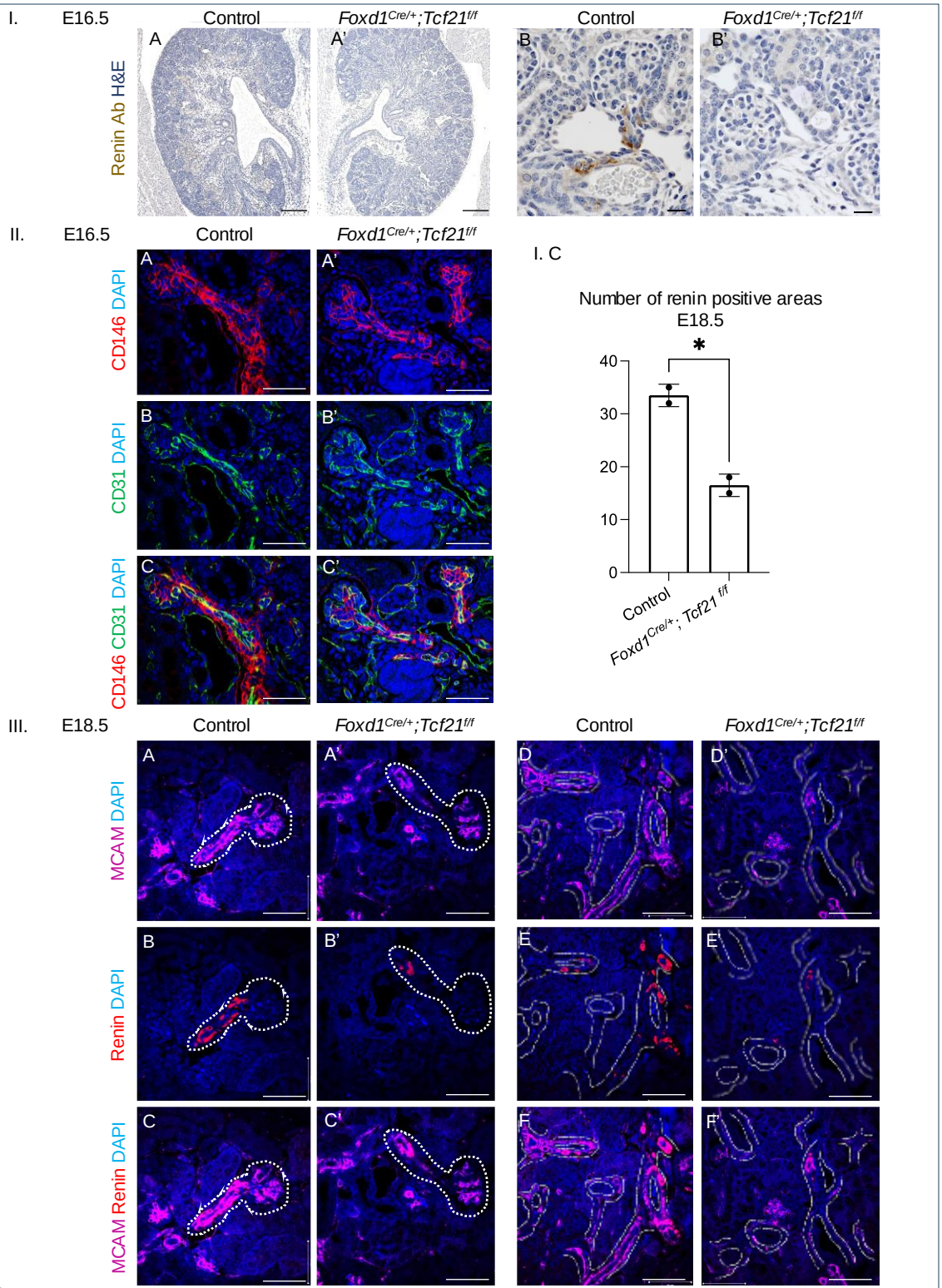
I.
E16.5
Control
Foxd1Cre/+;Tcf21f/f
Control
Foxd1Cre/+;Tcf21f/f
Renin Ab H&E
A
A'
B
B'
II.
E16.5
Control
Foxd1Cre/+;Tcf21f/f
CD146 DAPI
CD31 DAPI
CD146 CD31 DAPI
A
A'
B
B'
C
C'
I. C
Number of renin positive areas
E18.5
*
40
30
20
10
0
Control
Foxd1Cre/+; Tcf21 f/f
III.
E18.5
Control
Foxd1Cre/+;Tcf21f/f
Control
Foxd1Cre/+;Tcf21f/f
MCAM DAPI
Renin DAPI
MCAM Renin DAPI
A
A'
D
D'
B
B'
E
E'
C
C'
F
F'

Figure 1

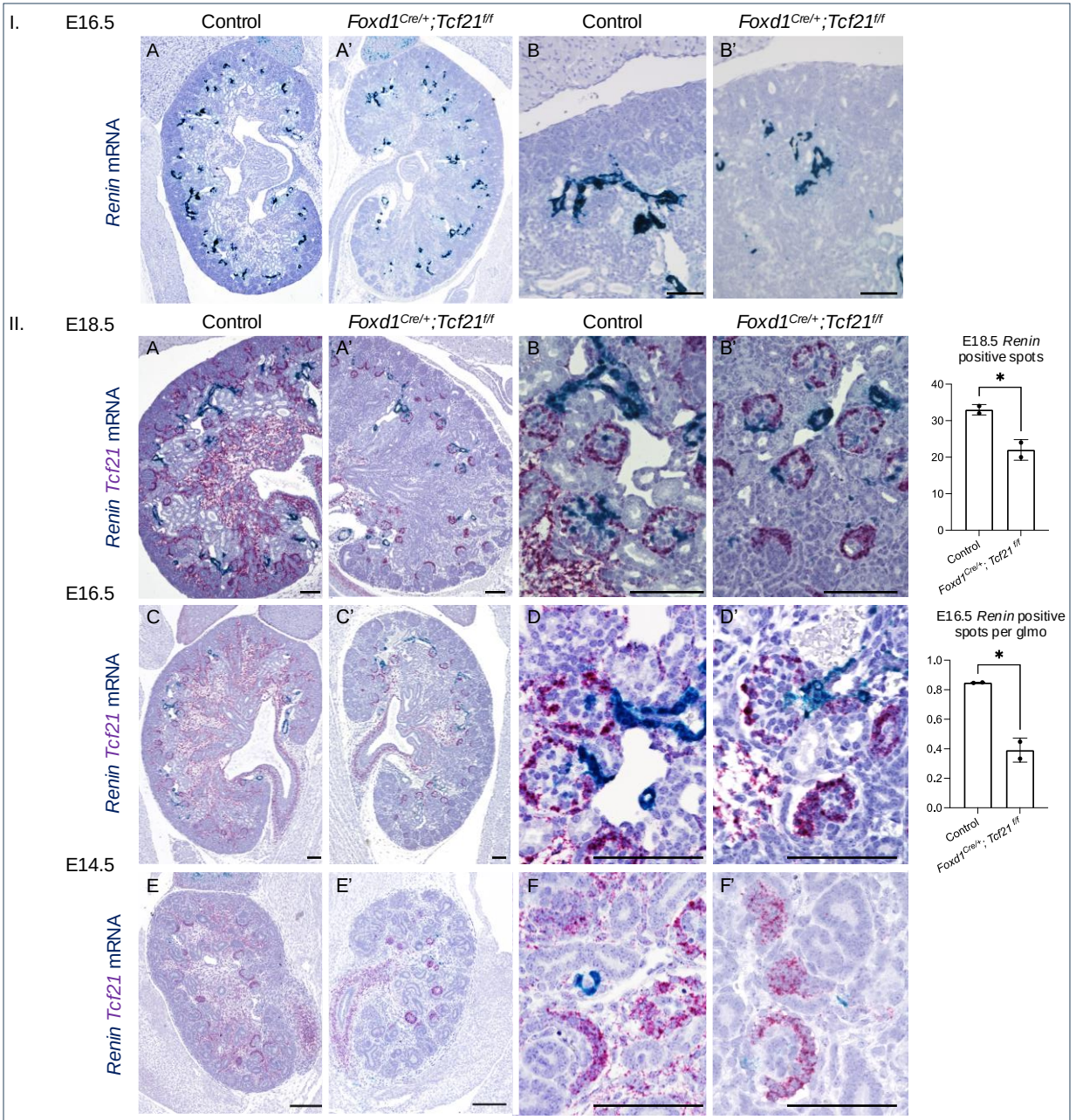
I.
E16.5
Control
Foxd1Cre/+;Tcf21f/f
Control
Foxd1Cre/+;Tcf21f/f
Renin mRNA
A
A'
B
B'
II.
E18.5
Control
Foxd1Cre/+;Tcf21f/f
Control
Foxd1Cre/+;Tcf21f/f
Renin Tcf21 mRNA
A
A'
B
B'
E18.5 Renin positive spots
40
30
20
10
0
*
Control
Foxd1Cre/+; Tcf21 f/f
E16.5
Renin Tcf21 mRNA
C
C'
D
D'
E16.5 Renin positive spots per glmo
1.0
0.8
0.6
0.4
0.2
0.0
*
Control
Foxd1Cre/+; Tcf21 f/f
E14.5
Renin Tcf21 mRNA
E
E'
F
F'

Figure 2

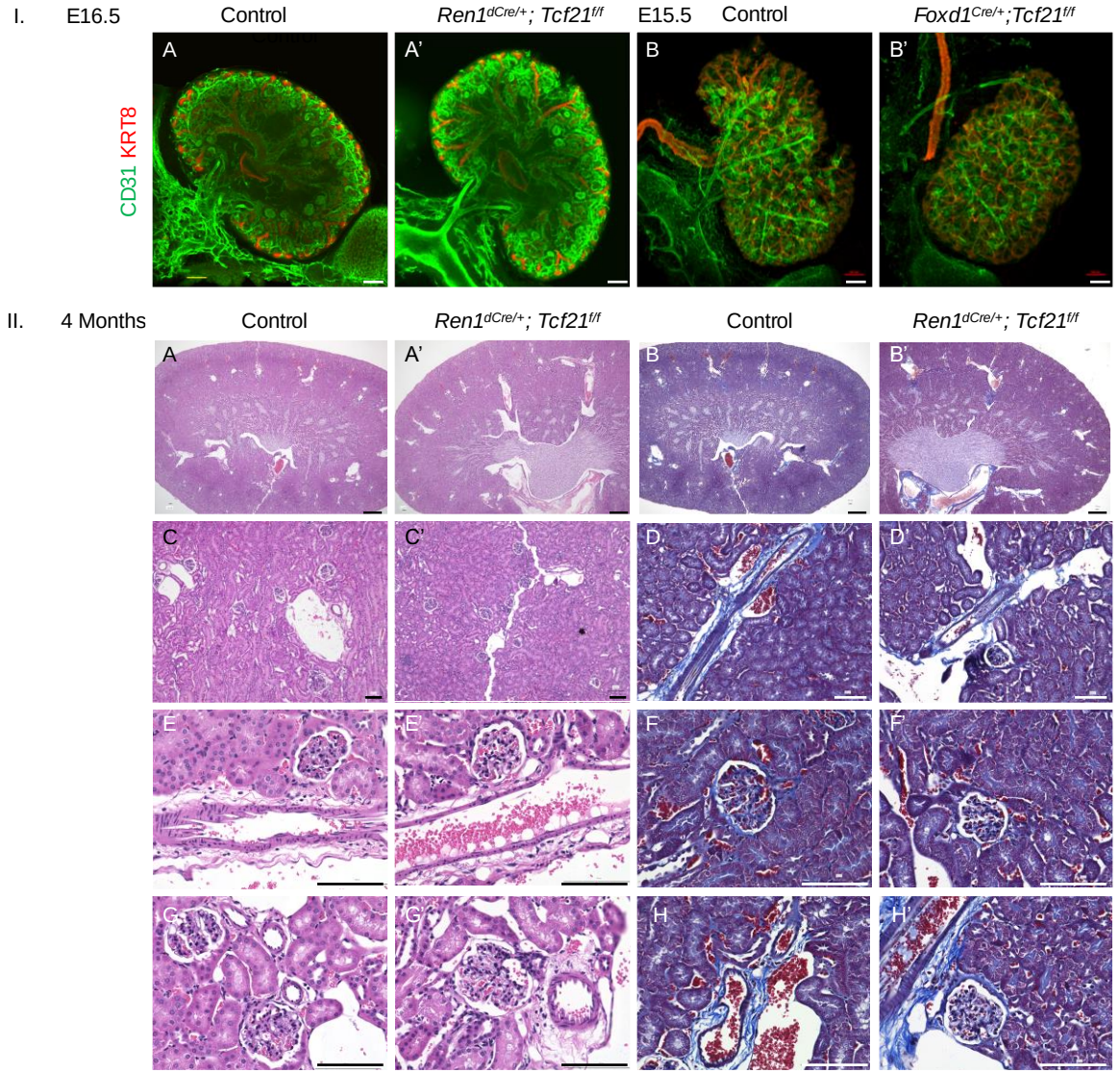
I.
E16.5
Control
Ren1dCre/+; Tcf21f/f
E15.5
Control
Foxd1Cre/+;Tcf21f/f
CD31 KRT8
A
A'
B
B'
II.
4 Months
Control
Ren1dCre/+; Tcf21f/f
Control
Ren1dCre/+; Tcf21f/f
A
A'
B
B'
C
C'
D
D'
E
E'
F
F'
G
G'
H
H'

Figure 3

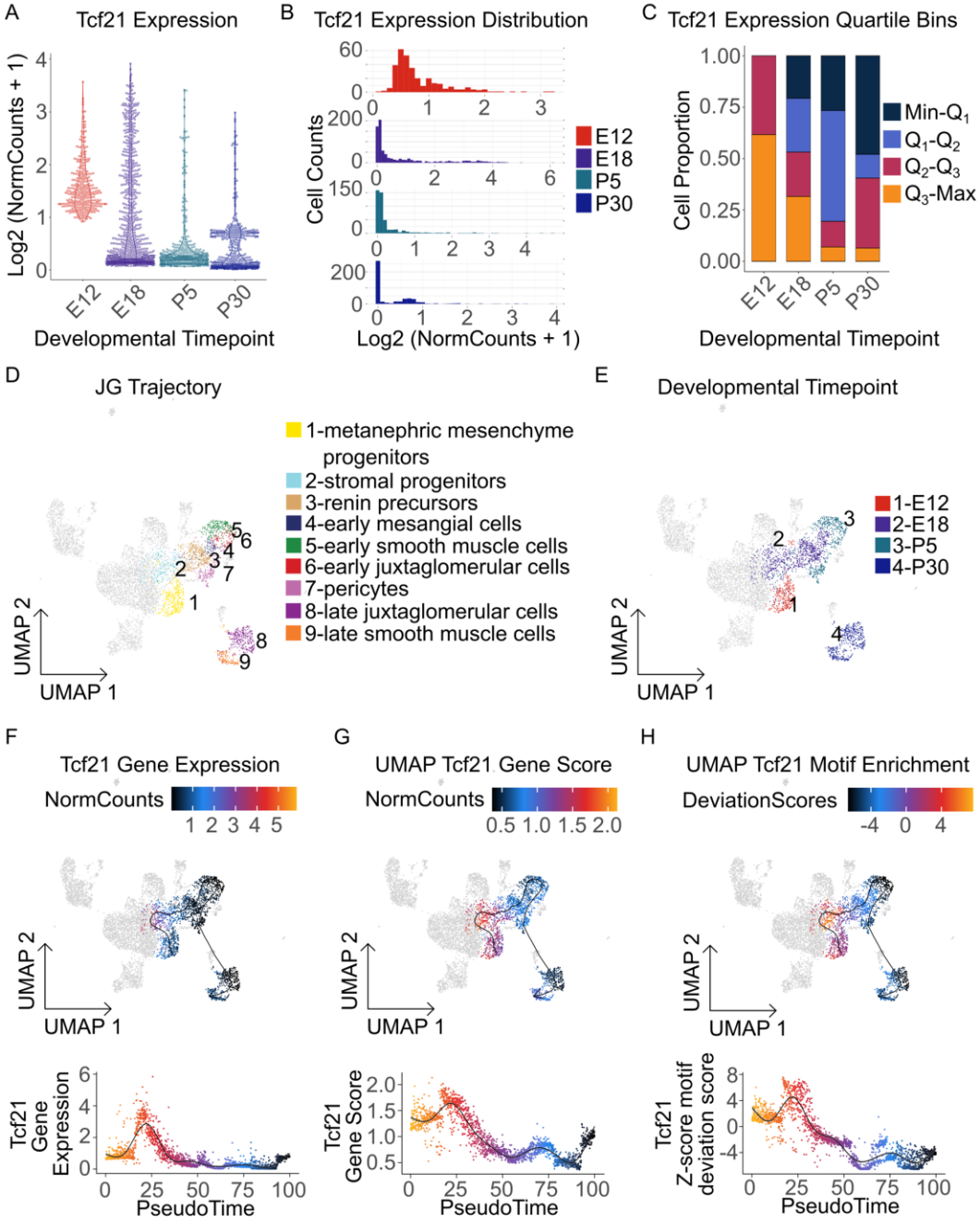
A
Tcf21 Expression
Log2 (NormCounts + 1)
E12
E18
P5
P30
Developmental Timepoint
B
Tcf21 Expression Distribution
Cell Counts
E12
E18
P5
P30
Log2 (NormCounts + 1)
C
Tcf21 Expression Quartile Bins
Cell Proportion
Min-Q1
Q1-Q2
Q2-Q3
Q3-Max
Developmental Timepoint
D
JG Trajectory
1-metanephric mesenchyme progenitors
2-stromal progenitors
3-renin precursors
4-early mesangial cells
5-early smooth muscle cells
6-early juxtaglomerular cells
7-pericytes
8-late juxtaglomerular cells
9-late smooth muscle cells
UMAP 2
UMAP 1
E
Developmental Timepoint
1-E12
2-E18
3-P5
4-P30
UMAP 2
UMAP 1
F
Tcf21 Gene Expression
NormCounts
UMAP 2
UMAP 1
Tcf21 Gene Expression
PseudoTime
G
UMAP Tcf21 Gene Score
NormCounts
UMAP 2
UMAP 1
Tcf21 Gene Score
PseudoTime
H
UMAP Tcf21 Motif Enrichment
DeviationScores
UMAP 2
UMAP 1
Tcf21 Z-score motif deviation score
PseudoTime

Figure 4